Angewandte Chemie
Eine Zeitschrift der Gesellschaft Deutscher Chemiker

Supporting Information

69451 Weinheim, Germany

Template-Induced Screw Motions within an Aromatic Amide Foldamer Double Helix**

Yann Ferrand, Quan Gan, Brice Kauffmann, Hua Jiang, and Ivan Huc**

ange_201101697_sm_miscellaneous_information.pdf

Table of contents

1. Material and methods

All reactions were carried out under a dry nitrogen atmosphere. Commercial reagents were purchased from Sigma-Aldrich or Alfa-Aesar and were used without further purification unless otherwise specified. Tetrahydrofurane (THF) and dichloromethane (DCM) were dried over alumina column; triethylamine (Et_3N) was distilled from calcium hydride (CaH_2) prior to use. Reactions were monitored by thin layer chromatography (TLC) on Merck silica gel 60-F254 plates and observed under UV light. Column chromatographies were carried out on Merck GEDURAN Si60 (40-63 µm). Melting points were measured on a Büchi B-540. ESI mass spectra were obtained on a Waters LCT Premier from the Mass Spectrometry Laboratory at the European Institute of Chemistry and Biology (UMS 3033 - IECB), Pessac, France. NMR spectra were recorded on 2 different NMR spectrometers: (1) an Avance II NMR spectrometer (Bruker Biospin) with a vertical 7,05T narrow-bore/ultrashield magnet operating at 300 MHz for ^{1}H observation and 75 MHz for ^{13}C observation by means of a 5-mm direct BBO H/X probe with Z gradient capabilities; (2) an Avance III NMR spectrometer (Bruker Biospin) with a vertical 16,45T narrow-bore/ultrashield magnet operating at 700 MHz for ^{1}H observation by means of a 5-mm TXI $^{1}H/^{13}C/^{15}N$ probe with Z gradient capabilities. Chemical shifts are reported in parts per million (ppm, δ) relative to the ^{1}H residual signal of the deuterated solvent used. ^{1}H NMR splitting patterns with observed first-order coupling are designated as singlet (s), doublet (d), triplet (t), or quartet (q). Coupling constants (*J*) are reported in hertz. Samples were not degassed. Data processing was performed with Topspin 2.0 software. Rotating-frame Overhauser spectroscopy (ROESY) experiments were recorded at 700 MHz and were used to distinguish dipolar interactions and exchange between free and bound double helices with the following acquisition parameters: the acquisition was performed with 2048(t2) x 512(t1) data points, in States-TPPI mode with Z gradients selection and with CW-spinlock for mixing, relaxation delay of 2 s, and 64 scans per increment; sweep width of 14000 Hz in both dimensions; mixing time of 300 ms. Processing was done after a sine-bell multiplication in both dimensions and Fourier transformation in 1K x 1K real points.

2. <u>Synthesis</u>

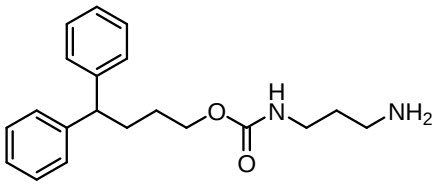

4,4-diphenylbutyl 3-aminopropylcarbamate 4. To a solution of 4-nitrophenyl chloroformate (1.1 g, 5.5 mmol) in dry CH_2Cl_2 (20 mL) was added dropwise a solution of 4,4-diphenylbutan-1-ol (1.1 g, 5.0 mmol) and Et_3N (2.8 mL, 20.0 mmol) in CH_2Cl_2 (10 mL) via a syringe at 0°C. After 30 min stirring at room temperature, the reaction mixture was added dropwise over a 1 h period to a solution of 1,3-diaminopropane (4.2 mL, 50.0 mmol) in dry CH_2Cl_2 (100 mL) at 0°C. Then the reaction mixture was allowed to proceed at room temperature for 12h. The solution was washed with 1N NaOH and brine several times, dried over Na_2SO_4. After filtration and concentration, the residual oil was purified by flash chromatography (SiO_2) eluting with MeOH/CH_2Cl_2/Et_3N (10:90:1 to 30:70:1) to obtain product **4** as yellow oil (1.32 g, 83% yield). ^{1}H NMR ($CDCl_3$, 300 MHz): δ 7.29-7.14 (m, 10H), 5.12 (br, 1H), 4.08 (t, *J*(H, H) = 6.6, 2H), 3.93 (t, *J*(H, H) = 7.8, 1H), 3.29 (q, *J*(H, H) = 6.0, *J*(H, H) = 6.6, 2H), 2.80 (t, *J*(H, H) = 6.6, 2H), 2.14 (q, *J*(H, H) = 7.8, *J*(H, H) = 7.8, 2H), 1.70 (br, 2H), 1.65-1.53 (m, 4H). ^{13}C NMR ($CDCl_3$, 75 MHz): δ 157.0, 144.7, 128.5, 127.8, 126.2, 64.6, 50.9, 39.1, 38.6, 32.1, 31.9, 27.6. HRMS (ES^+): *m/z* calcd for $C_{20}H_{26}N_2O_2$ $[M+H]^+$ 327.2073 found 327.2067.

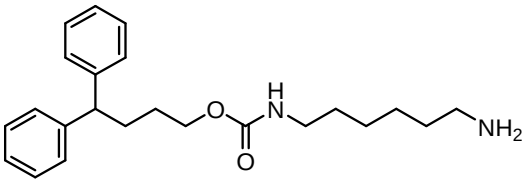

4,4-diphenylbutyl 6-aminohexylcarbamate 5. To a solution of 4-nitrophenyl chloroformate (0.35 g, 1.7 mmol) in dry CH_2Cl_2 (20 mL) was added dropwise a solution of 4,4-diphenylbutan-1-ol (0.36 g, 1.6 mmol) and Et_3N (0.89 mL, 6.4 mmol) in CH_2Cl_2 (10 mL) via a syringe at 0°C. After 30 min stirring at room temperature, the reaction mixture was added dropwise over a 1 h period to a solution of 1,6-diaminohexane (0.93 g, 8.0 mmol) in dry CH_2Cl_2 (100 mL) at 0°C. Then the reaction mixture was allowed to proceed at room temperature for 12h. The solution was washed with 1N NaOH and brine several times, dried over Na_2SO_4. After filtration and concentration, the residual oil was purified by flash chromatography (SiO_2) eluting with MeOH/CH_2Cl_2/Et_3N (10:90:1 to 30:70:1) to obtain product **5** as yellow oil (0.47 g, 80% yield). ^{1}H NMR ($CDCl_3$, 300 MHz): δ 7.30-7.14 (m, 10H), 4.62 (br, 1H), 4.08 (t, *J*(H, H) = 6.3, 2H), 3.93 (t, *J*(H, H) = 7.8, 1H), 3.17 (q,

J(H, H) = 6.6, *J*(H, H) = 6.6, 2H), 2.68 (br, 2H), 2.14 (q, *J*(H, H) = 7.8, *J*(H, H) = 7.8, 2H), 1.60-1.32 (m, 12H). ^{13}C NMR ($CDCl_3$, 75 MHz): δ 156.8, 144.8, 128.6, 127.9, 126.3, 64.7, 51.1, 42.1, 41.0, 32.0, 30.1, 27.7, 26.6, 26.6. HRMS (ES^+): *m/z* calcd for $C_{23}H_{32}N_2O_2$ $[M+H]^+$ 369.2542 found 369.2529.

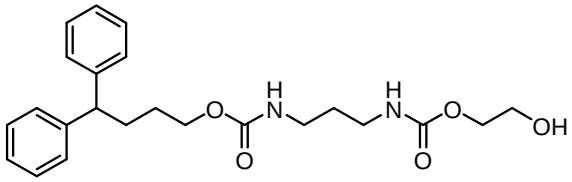

Compound 6. To a solution of 4-nitrophenyl chloroformate (0.734 g, 3.6 mmol) in dry CH_2Cl_2 (20 mL) was added dropwise a solution of 4,4-diphenylbutyl 6-aminohexylcarbamate (1.08 g, 3.3 mmol) and Et_3N (1.83 mL, 13.2 mmol) in CH_2Cl_2 (10 mL) via a syringe at 0°C. After 30 min stirring at room temperature, the above reaction mixture was added dropwise over a 1 h period to a solution of ethylene glycol (9.2 mL, 0.16 mol) in dry THF (100 mL) at 0°C. Then the reaction mixture was allowed to proceed at room temperature for 12h. The solution was washed with 1N NaOH and brine several times, dried over Na_2SO_4. After filtration and concentration, the residual oil was purified by flash chromatography (SiO_2) eluting with EtOAc/CH_2Cl_2 (20:80 to 60:40) to obtain product **6** as colourless oil (0.58 g, 42% yield). ^{1}H NMR ($CDCl_3$, 300 MHz): δ 7.30-7.15 (m, 10H), 5.39 (br, 1H), 5.04 (br, 1H), 4.20 (t, *J*(H, H) = 4.2, 2H), 4.08 (t, *J*(H, H) = 6.6, 2H), 3.93 (t, *J*(H, H) = 7.8, 1H), 3.80 (t, *J*(H, H) = 4.2, 2H), 3.24-3.18 (m, 4H), 2.52 (br, 1H), 2.14 (q, *J*(H, H) = 7.8, *J*(H, H) = 7.8, 2H), 1.67-1.55 (m, 4H). ^{13}C NMR ($CDCl_3$, 75 MHz): δ 157.5, 157.3, 144.8, 128.6, 127.9, 126.3, 66.9, 65.0, 61.9, 51.1, 37.7, 37.6, 32.0, 30.5, 27.7. HRMS (ES^+): *m/z* calcd for $C_{23}H_{30}N_2NaO_5$ $[M+Na]^+$ 437.2052 found 437.2045.

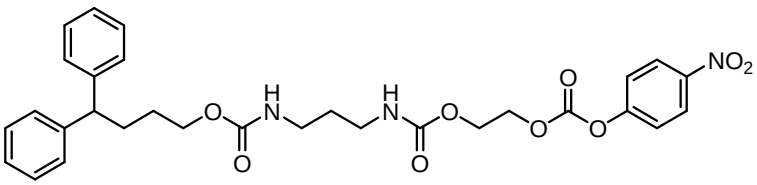

Compound 7. To a solution of 4-nitrophenyl chloroformate (0.21 g, 1.06 mmol) in dry CH_2Cl_2 (20 mL) was added dropwise a solution of **6** (0.4 g, 0.97 mmol) and Et_3N (0.54 mL, 3.86 mmol) in CH_2Cl_2 (10 mL) via a syringe at 0°C. Then the reaction mixture was allowed to proceed at room temperature for 2h. The solution was evaporated and the residual oil was purified by flash chromatography (SiO_2) eluting with EtOAc/CH_2Cl_2 (10:90 to 30:70) to obtain product **7** as colourless oil (0.50 g, 88% yield). ^{1}H NMR ($CDCl_3$, 300 MHz): δ 8.30-8.25 (m, 2H), 7.41-7.38 (m,

2H), 7.30-7.14 (m, 10H), 5.32 (br, 1H), 4.93 (br, 1H), 4.48-4.45 (m, 2H), 4.38-4.36 (m, 2H), 4.08 (t, *J*(H, H) = 6.6, 2H), 3.93 (t, *J*(H, H) = 7.8, 1H), 3.26-3.20 (m, 4H), 2.14 (q, *J*(H, H) = 7.8, *J*(H, H) = 7.8, 2H), 1.68-1.53 (m, 4H). ^{13}C NMR ($CDCl_3$, 75 MHz): δ 157.2, 156.3, 155.3, 152.3, 145.3, 144.6, 128.4, 127.7, 126.1, 125.2, 121.7, 67.4, 64.7, 61.9, 50.8, 37.5, 37.3, 31.8, 30.2, 27.5. HRMS (ES^+): *m/z* calcd for $C_{30}H_{33}N_3NaO_9$ $[M+Na]^+$ 602.2114 found 602.2063.

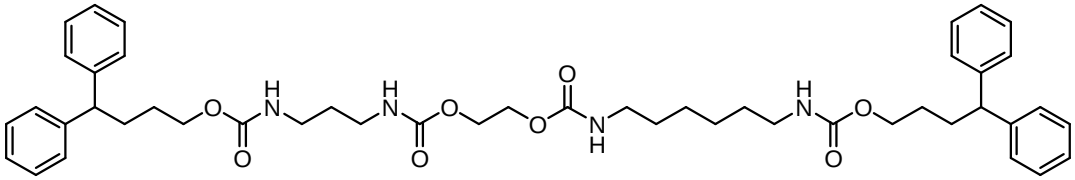

Rod 3. To compound **7** (0.33 g, 0.58 mmol) in dry CH_2Cl_2 (10 mL) was added dropwise a solution of 4,4-diphenylbutyl 6-aminohexylcarbamate (0.21 g, 0.58 mmol) and Et_3N (0.32 mL, 2.3 mmol) in CH_2Cl_2 (10 mL) via a syringe at 0°C. Then the reaction mixture was allowed to proceed at room temperature for 12h. The solution was washed with 1N NaOH and brine several times, dried over Na_2SO_4. After filtration and concentration, the residual oil was purified by flash chromatography (SiO_2) eluting with EtOAc/CH_2Cl_2 (20:80 to 50:50) to obtain product **3** as a white solid (0.39 g, 84% yield). ^{1}H NMR ($CDCl_3$, 300 MHz): δ 7.30-7.14 (m, 20H), 5.18 (br, 1H), 5.04 (br, 1H), 4.81 (br, 1H), 4.67 (br, 1H), 4.23 (br, 4H), 4.08 (t, *J*(H, H) = 6.6, 4H), 3.93 (t, *J*(H, H) = 7.8, 2H), 3.23-3.12 (m, 8H), 2.14 (q, *J*(H, H) = 7.8, *J*(H, H) = 7.8, 4H), 1.66-1.53 (m, 6H), 1.47-1.45 (m, 4H), 1.31 (br, 4H). ^{13}C NMR ($CDCl_3$, 75 MHz): δ 157.2, 156.8, 156.7, 156.3, 144.8, 144.7, 128.5, 127.8, 126.3, 64.8, 64.6, 63.2, 63.1, 51.0, 40.9, 40.8, 37.6, 37.5, 31.9, 30.4, 29.9, 29.8, 27.7, 26.3. HRMS (ES^+): *m/z* calcd for $C_{47}H_{60}N_4NaO_8$ $[M+H]^+$ 831.4309 found 831.4313. m.p.: 101.5.-102.3°C.

S3. ^{1}H NMR Spectroscopy

Determination of association constant (K_a)

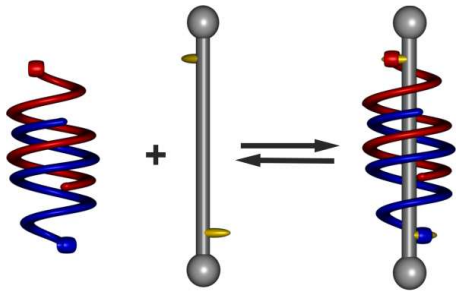

For the equilibrium shown in Eq. 1, the association constant K_a of the double helix DH is given by Eq. 2.

$$DH + R \rightleftharpoons F \qquad (1)$$

$$K_a = \frac{[F]}{[DH][R]} \qquad (2)$$

where: [F] = foldaxane concentration; [DH] = double helix concentration; [R] = rod concentration

Alternatively, $$K_a = \frac{n_F \times V_T}{n_{DH} \times n_R} \qquad (3)$$

where: V_T = total volume of the sample; n_H = number of moles of double helix

From mass balance, $$n_{DH_0} = n_{DH} + n_F \qquad (4)$$

$$n_{R_0} = n_R + n_F \qquad (5)$$

where: n_{DH0} = initial number of moles of double helix; n_{R0} = number of moles of rod added to the sample

Substituting equations (4) and (5) into (3), $$K_a = \frac{n_F \times V_T}{(n_{DH_0} - n_F) \times (n_{R_0} - n_F)} \qquad (6)$$

From integration of the NMR spectrum it is possible to obtain the fraction of bound DH host, x (Eq. 7).

$$x = \frac{n_F}{n_{DH_0}} \qquad (7)$$

Using Eq. 7 to eliminate n_{HG} from Eq. 6, $$K_a = \frac{x \times V_T}{n_{R_0} - (x \times n_{DH_0}) - (x \times n_{R_0}) + (x^2 \times n_{DH_0})} \qquad (8)$$

The fraction of bound double helices x (Eq. 7) was found by integration of the region of NH amide δ 9.5-11.5 ppm of the NMR spectra shown in Figure S1 to S4. This region contains the signal for NH amide protons of free double helix and for NH amide foldaxane protons (for labelling see Fig. S1-S4). Eq. 8 was then used to calculate K_a from each spectrum. The resulting K_a values (averaged) are shown in Table S1.

Table S1. Titration of oligomer **1** by different dumbbell molecules monitored by NMR (300 MHz) in $CDCl_3$ at 298K. Dashes reflect no affinity of the oligomers for the rods. All experimental errors < 5%. K_a in $L.mol^{-1}$.

	2a	**2b**	**2c**	**2d**	**2e**	**2f**
$(\mathbf{1})_2$	-	55	20	140	35	-

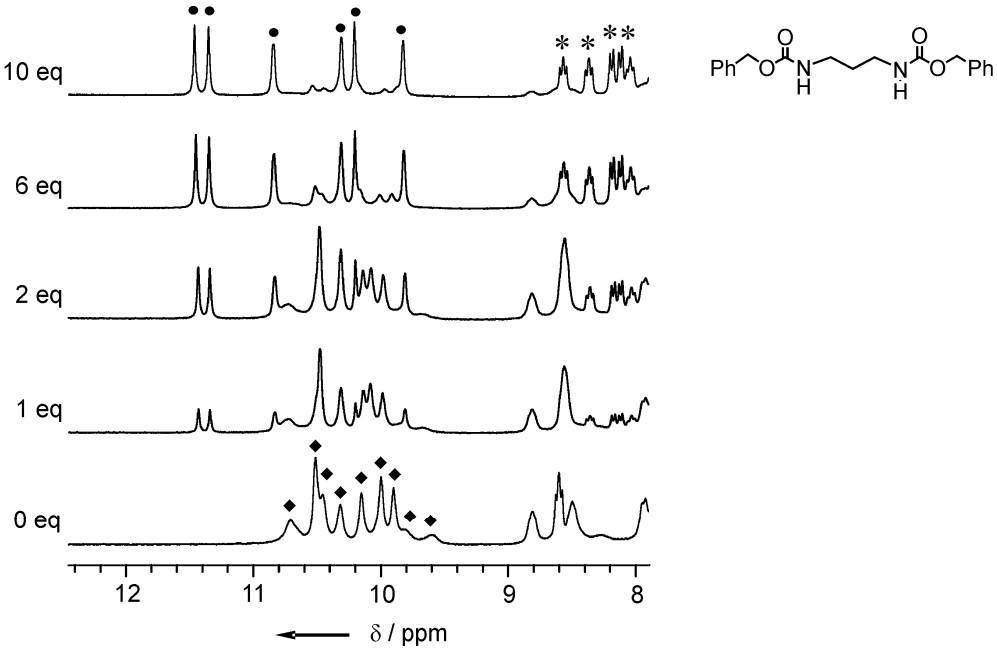

Figure S1. Representative 300 MHz NMR spectra of **1** (8 mM) in $CDCl_3$ titrated with **2b**. Amide signals of the free double helix and foldaxane are marked with diamonds and black circles, respectively. Aromatic proton resonances are marked with stars. Ka = 55 L mol^{-1}.

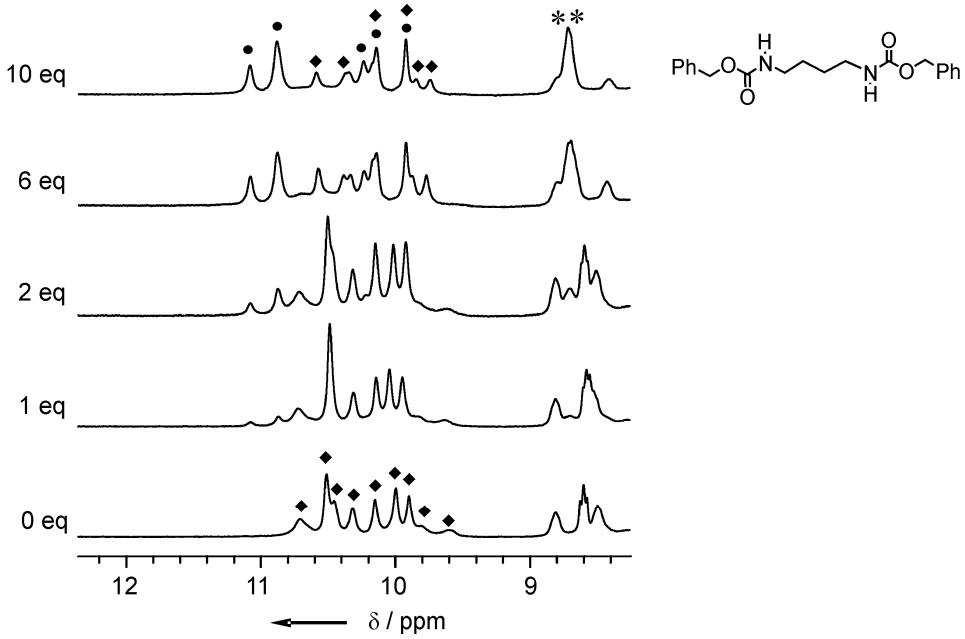

Figure S2. Representative 300 MHz NMR spectra of **1** (8 mM) in $CDCl_3$ titrated with **2c**. Amide signals of the free double helix and foldaxane are marked with diamonds and black circles, respectively. Aromatic proton resonances are marked with stars. Ka = 20 $L.mol^{-1}$.

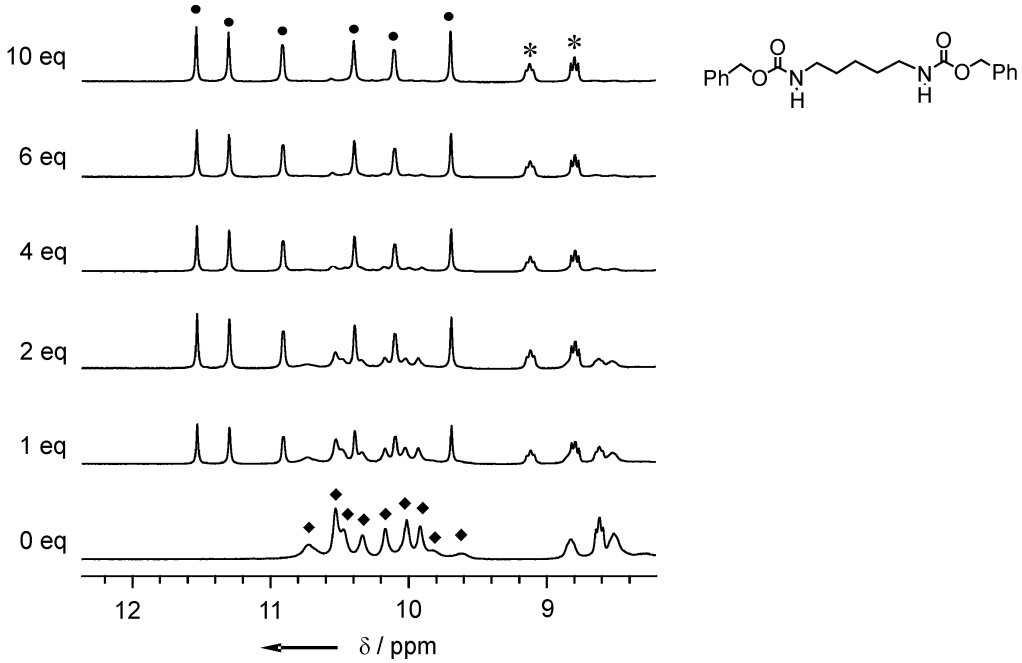

Figure S3. Representative 300 MHz NMR spectra of **1** (8 mM) in $CDCl_3$ titrated with **2d**. Amide signals of the free double helix and foldaxane are marked with diamonds and black circles, respectively. Aromatic proton resonances are marked with stars. Ka = 140 $L.mol^{-1}$.

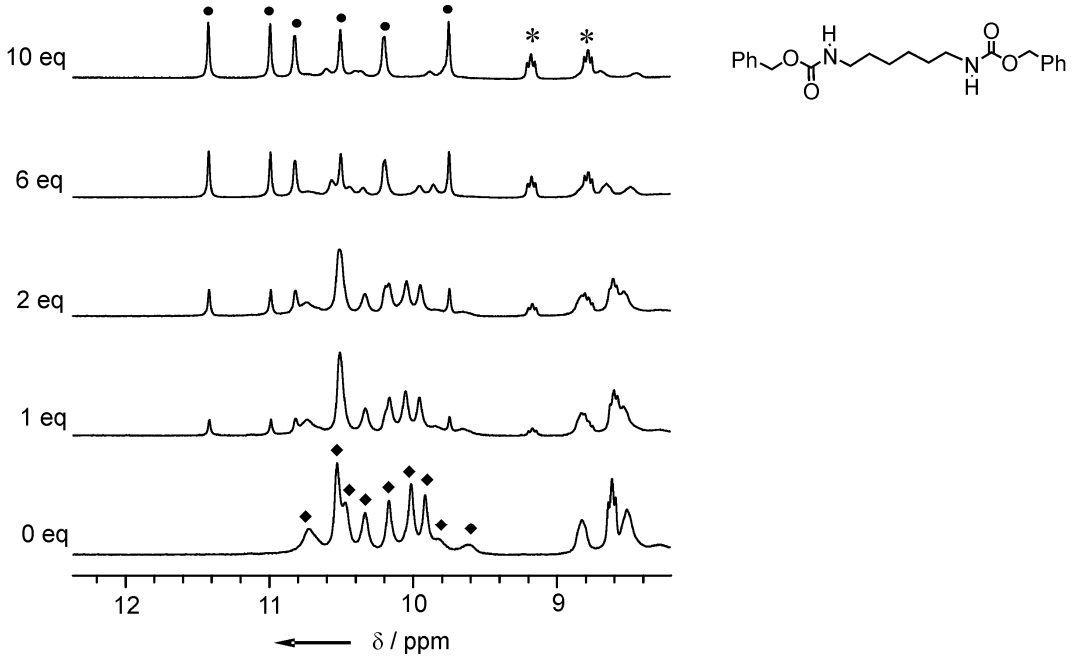

Figure S4. Representative 300 MHz NMR spectra of **1** (8 mM) in $CDCl_3$ titrated with **2e**. Amide signals of the free double helix and foldaxane are marked with diamonds and black circles, respectively. Aromatic proton resonances are marked with stars. K_a = 35 L.mol^{-1}.

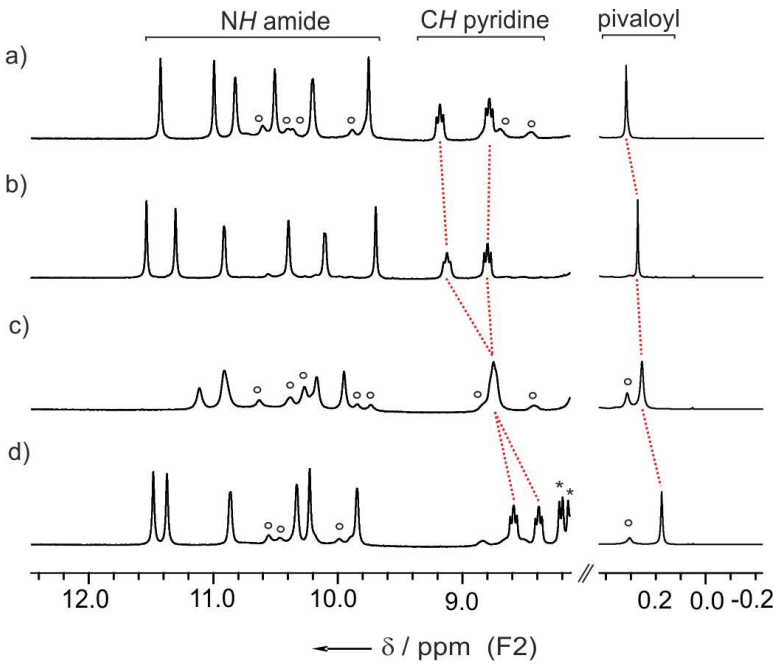

Figure S5. 300 MHz NMR spectra of **1** (8 mM) in $CDCl_3$ titrated with a) **2e** (10 equiv.); b) **2d** (10 equiv.); c) **2c** (20 equiv.); d) **2b** (10 equiv.). Unlabeled signals are those of the foldaxanes. Circles denote residual signals of $(\mathbf{1})_2$. The resonances of pivaloyl protons and of pyridine protons in position 4 shift to higher fields when the guest is shortened, consistent with the screwing of the two strands into one another, resulting in an increased ring current effect. In contrast, NH amide protons which converge towards the helix cavity do not shift.

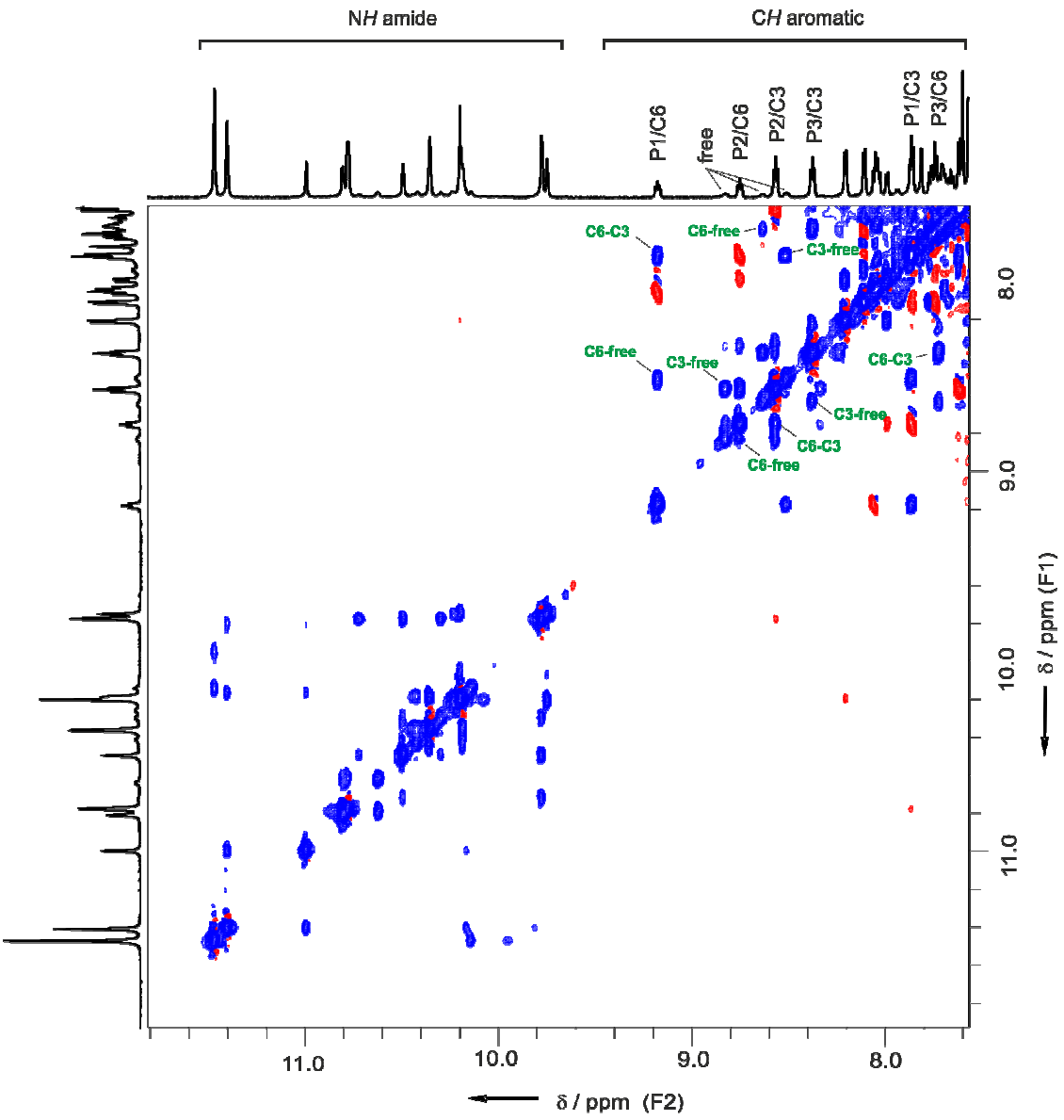

Figure S6. Expansion of the ^{1}H-^{1}H ROESY spectrum at 4°C (700 MHz) of (**1**)$_2$ (8 mM) in the presence of **2b** and **2e** (10 equiv. each) recorded with 300ms mixing time. Intense cross peaks show that protons of the free double helix (**1**)$_2$, (**1**)$_2$⊃**2b** and (**1**)$_2$⊃**2e** complex exchange in a slow exchange regime on the NMR time scale. NOEs cross peaks are observed in red whereas exchange peaks are seen in blue. Some exchanges cross peaks have been labelled in green. P1, P2, P3 denote protons belong to independent pyridine spin systems but have not been assigned to each pyridine rings in the sequence. C3 or C6 denotes the number (3 or 6) of CH_2 units of the alkyl chain of the guest on which the double helix resides

4. X-Ray Crystallography

Mode of binding

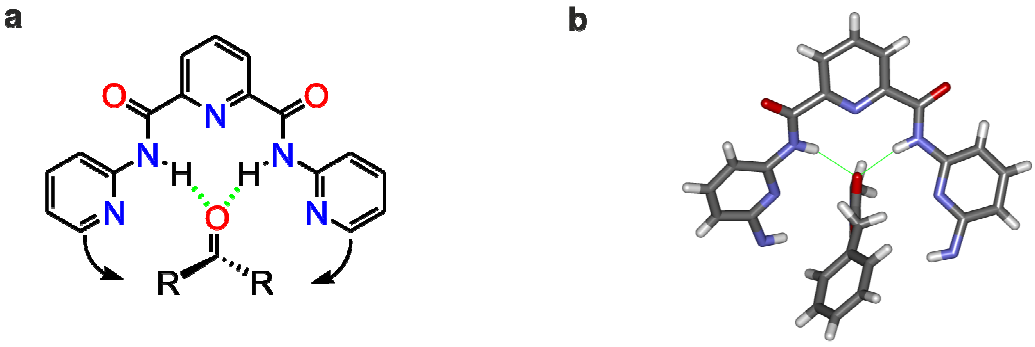

Figure S5. a) Schematic representation showing that the 2,6-pyridinedicarboxamide units of the helices hydrogen bond to the carbonyl groups of the guests. b) Slice of the crystal structure of **1⊃2d** confirming the expected pattern. Each carbonyl moiety is doubly hydrogen bonded ($d_{NH...OC}$ = 2.93 Å, $d_{NH...OC}$ = 2.89 Å) to a neighboring N*H* amide of 2,6-pyridinedicarboxamide.

The data for crystal structures of compounds (**1**)$_2$⊃**2b**, (**1**)$_2$⊃**2e** and (**1**)$_2$⊃**2e**, have been collected at the European Institute for Chemistry and Biology X-ray facility (UMS 3033) on a Bruker X8 proteum rotating anode at the CuK radiation wavelength. The system features the microstar micro-focus x-ray source with the PLATINUM135 CCD detector combined with the 4-circle KAPPA goniometer and the Helios multilayer graded optics. The system is driven by the PROTEUM2 software (S1). The unit cells determinations have been performed using a combination of Fast Fourier and Difference Vector techniques, the data were integrated using SAINT and scaled and corrected for absorption with SADABS. All the structures have been solved by direct methods with SHELXD and refined by full-matrix least-squares methods using SHELXL (S2). The WinGX-software (S3) was used for modelling. It has to be noticed that all the crystals described below contain a large percentage of disordered solvent molecules and very few of them could be modeled in the Fourier difference density maps. High flux X-ray Beams on small crystals with high solvent contents can explain the modest quality of the refinement statistics reported in this study.

References:

S1. Proteum II suite Bruker AXS version 2005.

S2. G. M. Sheldrick, Acta Cryst. A64, 112 (2008).

S3. L. J. Farrugia, J. Appl. Cryst. 32, 837 (1999).

- X-Ray crystallographic data for antiparallel double helix (**1**)$_2$⊃**2b**

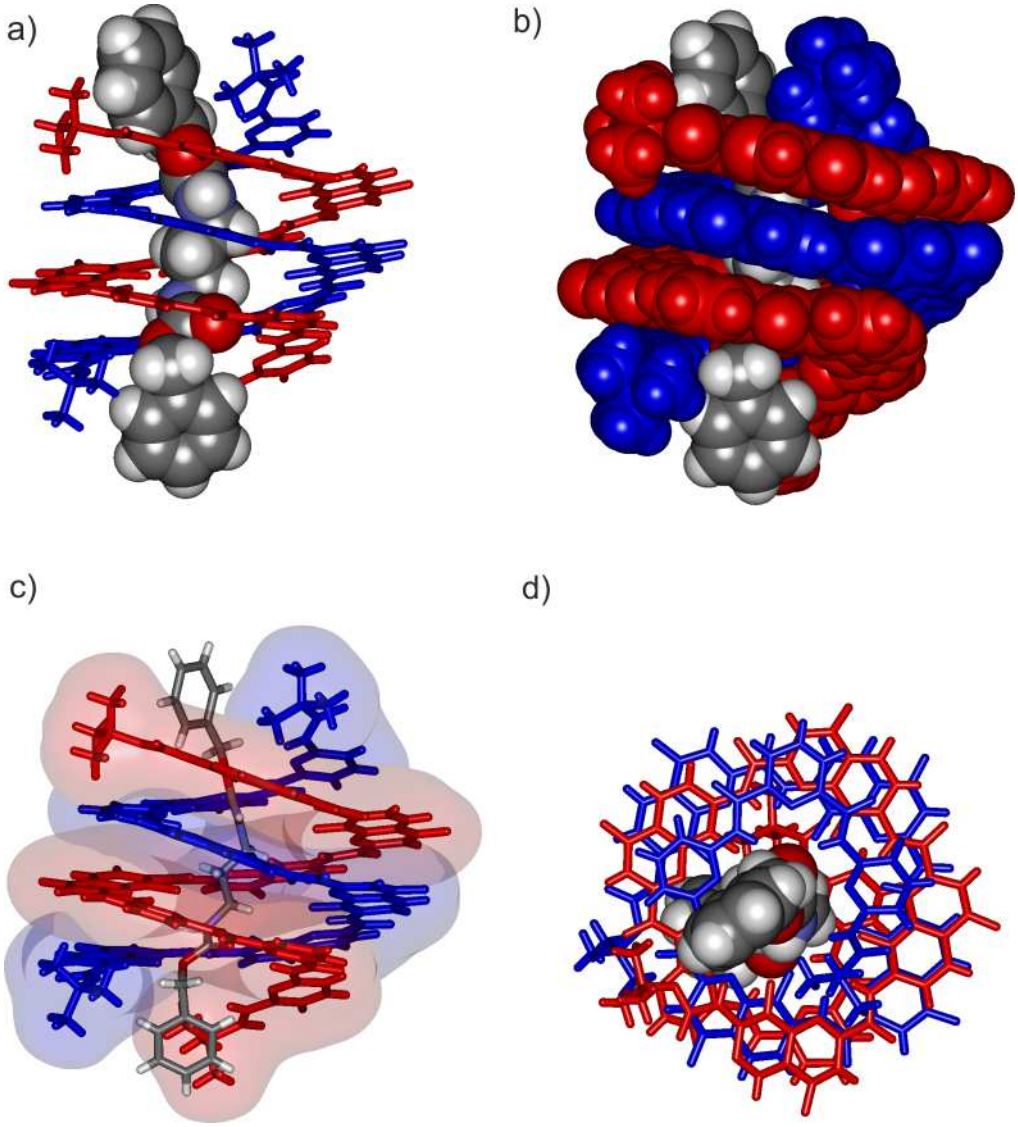

Figure S6. a) Side view (rod in CPK and double helix in tube representation); b) top view (both double helix and rod in CPK representation) and c) side view of the crystal structures of the foldaxane (**1**)$_2$⊃**2b** in tube representation with solvent accessible surfaces. d) Top view of (**1**)$_2$⊃**2b** (double helix in tube representation and rod in CPK representation). Isobutyl side chains and included solvent molecules have been removed for clarity.

Table S3: Crystal data and structure refinement for double helix (**1**)$_2$⊃**2b**.

Formula	$C_{97}H_{96}Cl_9F_4N_{16}O_{17.5}$
M	2160.95
Crystal system	Triclinic
Space group	P-1
a/Å	19.909(4)
b/Å	21.829(4)
c/Å	25.945(4)
α/o	78.12(3)
β/°	84.31(3)
γ/°	78.30(4)
V/Å^3	10785
T /K	213
Z	4
ρ/g cm^{-1}	1.331
size (mm)	0.1x0.05x0.05
λ/ Å	1.54178
μ/mm^{-1}	2.782
Absorption correction	no
unique data	21169
parameters/restraints	2586/12
R1, wR2	0.1126, 0.3815
goodness of fit	1.824
CCDC #	816152

- X-Ray crystallographic data for antiparallel double helix (**1**)$_2$⊃**2d**

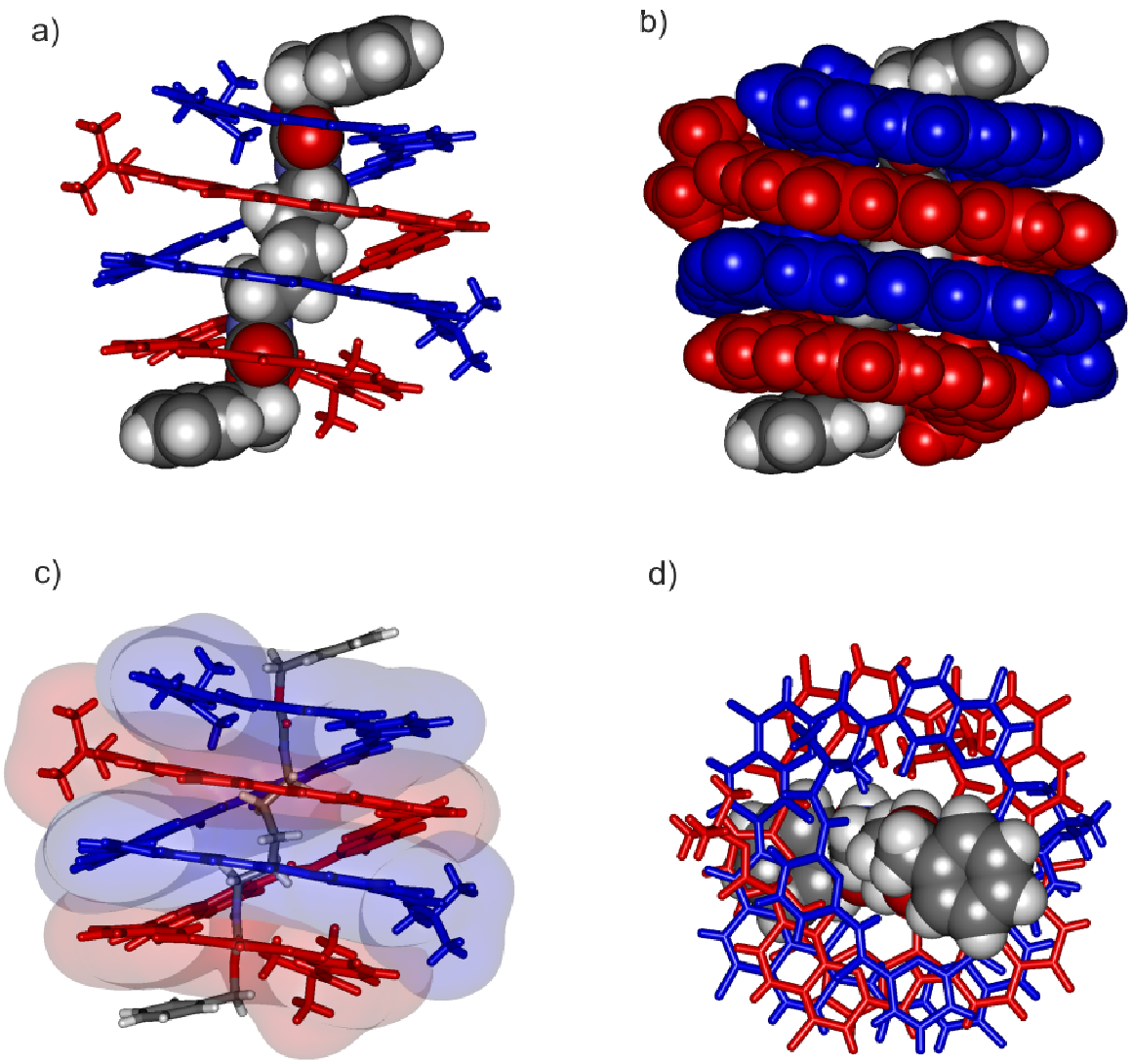

Figure S7. a) Side view (rod in CPK and double helix in tube representation); b) top view (both double helix and rod in CPK representation) and c) side view of the crystal structures of the foldaxane (**1**)$_2$⊃**2d** in tube representation with solvent accessible surfaces. d) Top view of (**1**)$_2$⊃**2d** (double helix in tube representation and rod in CPK representation). Isobutyl side chains and included solvent molecules have been removed for clarity.

Table S4: Crystal data and structure refinement for double helix $(\mathbf{1})_2 \supset \mathbf{2d}$.

Formula	$C_{196}H_{206}Cl_{17.91}F_8N_{31}O_{34.5}$
M	3980.4
Crystal system	Triclinic
Space group	P-1
a/Å	17.764(4)
b/Å	21.407(4)
c/Å	30.835(4)
α/°	101.31(3)
β/°	100.24(3)
γ/°	112.31(3)
V/Å^3	10219
T /K	213
Z	2
ρ/g cm^{-1}	1.294
size (mm)	0.05x0.02x0.02
λ/ Å	1.54178
μ/mm^{-1}	1.702
Absorption correction	no
unique data	15775
parameters/restraints	2426/44
R1, wR2	0.1869, 0.4340
goodness of fit	1.135
CCDC #	816315

- X-Ray crystallographic data for antiparallel double helix (**1**)$_2$⊃**2e**

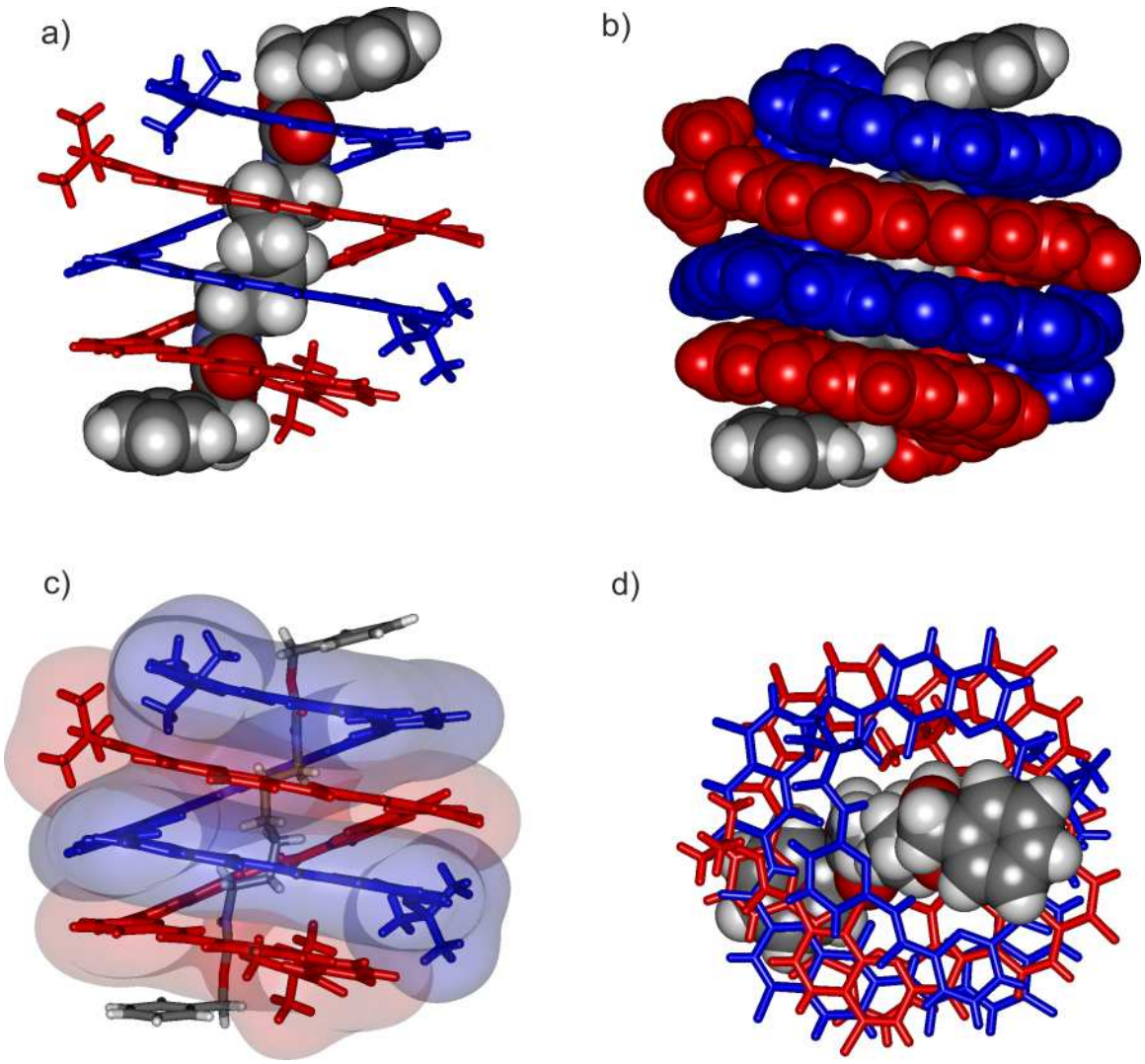

Figure S8. a) Side view (rod in CPK and double helix in tube representation); b) top view (both double helix and rod in CPK representation) and c) side view of the crystal structures of the foldaxane (**1**)$_2$⊃**2e** in tube representation with solvent accessible surfaces. c) Top view of (**1**)$_2$⊃**2e** (double helix in tube representation and rod in CPK representation). Isobutyl side chains and included solvent molecules have been removed for clarity.

Table S5: Crystal data and structure refinement for double helix (**1**)$_2$⊃**2e**.

Formula	$C_{195}H_{201}Cl_{21}F_8N_{32}O_{46.75}$
M	4637.34
Crystal system	Triclinic
Space group	P-1
a/Å	17.995(4)
b/Å	23.036(5)
c/Å	31.217(6)
α/°	74.79(3)
β/°	81.13(3)
γ/°	78.79(3)
V/Å^3	12152
T /K	213
Z	2
ρ/g cm^{-1}	1.267
size (mm)	0.1x0.05x0.05
λ/ Å	1.54178
μ/mm^{-1}	2.838
Absorption correction	No
unique data	19696
parameters/restraints	2646/22
R1, wR2	0.1796, 0.4477
goodness of fit	1.914
CCDC #	816316

5. ^{1}H and ^{13}C NMR spectra

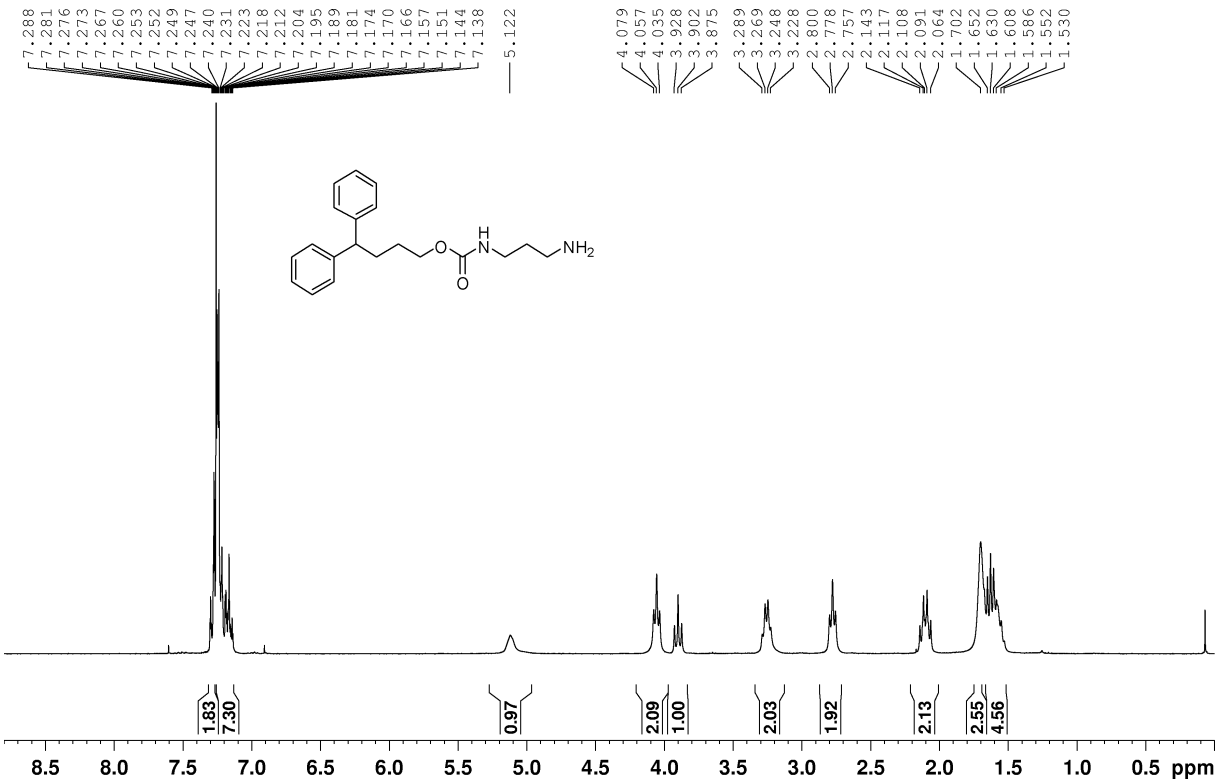

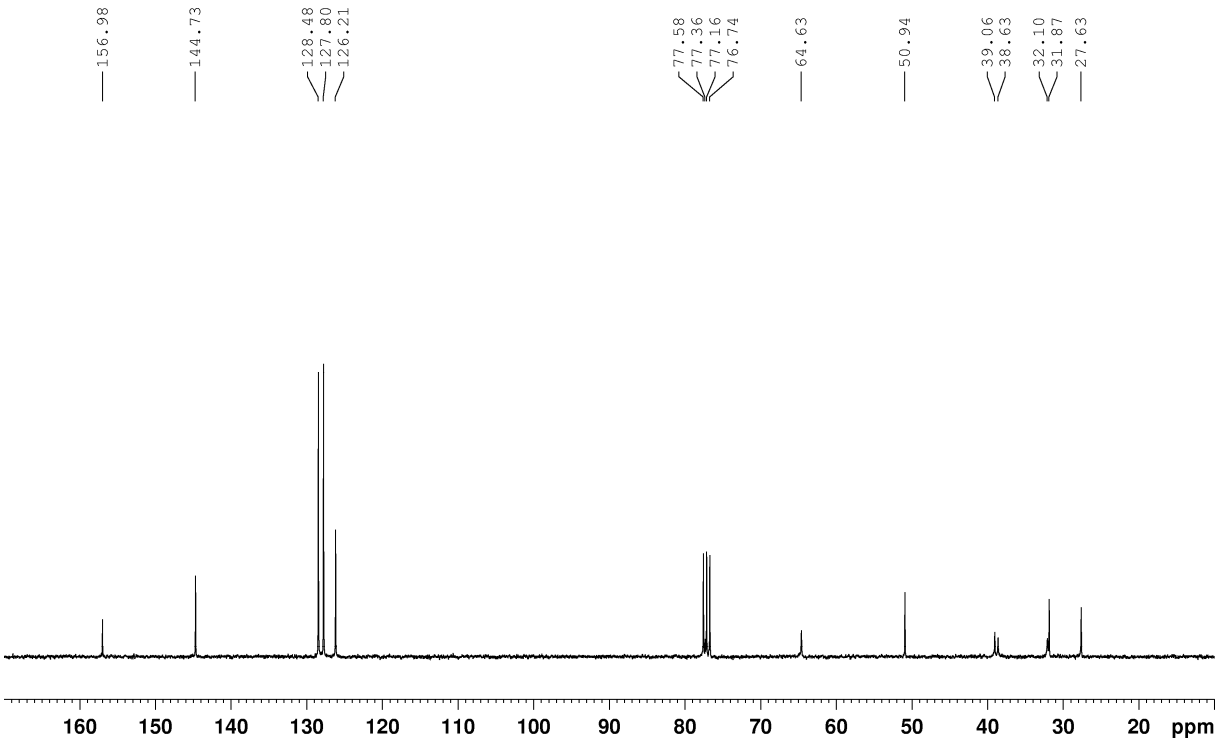

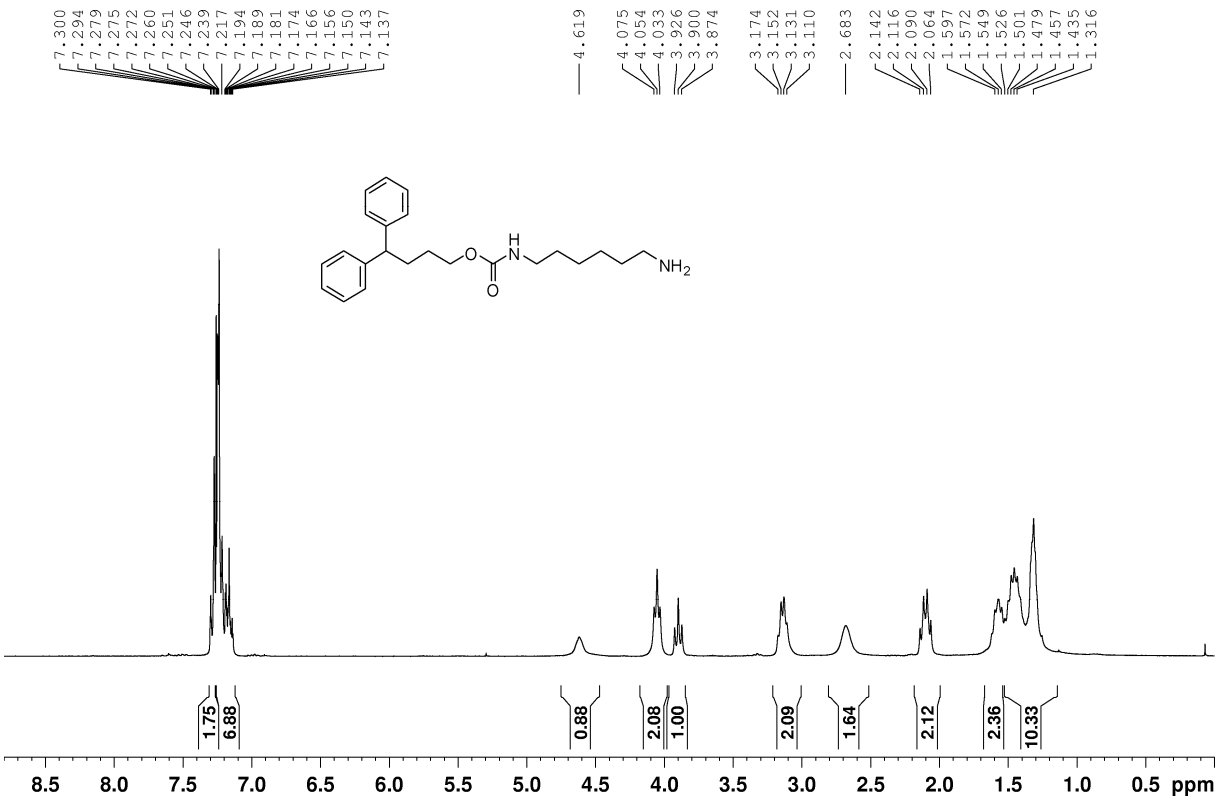
7.300
7.294
7.279
7.275
7.272
7.260
7.251
7.246
7.239
7.217
7.194
7.189
7.181
7.174
7.166
7.156
7.150
7.143
7.137
4.619
4.075
4.054
4.033
3.926
3.900
3.874
3.174
3.152
3.131
3.110
2.683
2.142
2.116
2.090
2.064
1.597
1.572
1.549
1.526
1.501
1.479
1.457
1.435
1.316
O
H
N
O
NH2
1.75
6.88
0.88
2.08
1.00
2.09
1.64
2.12
2.36
10.33
8.5
8.0
7.5
7.0
6.5
6.0
5.5
5.0
4.5
4.0
3.5
3.0
2.5
2.0
1.5
1.0
0.5
ppm

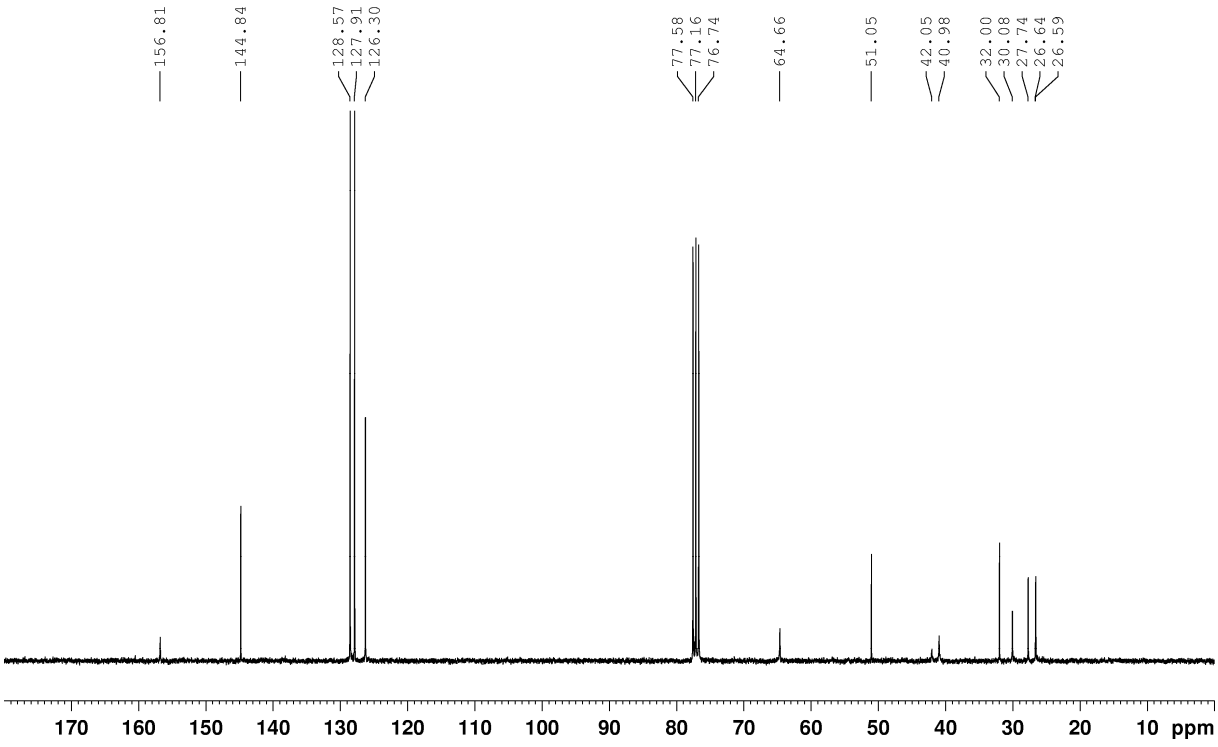
156.81
144.84
128.57
127.91
126.30
77.58
77.16
76.74
64.66
51.05
42.05
40.98
32.00
30.08
27.74
26.64
26.59
170
160
150
140
130
120
110
100
90
80
70
60
50
40
30
20
10
ppm

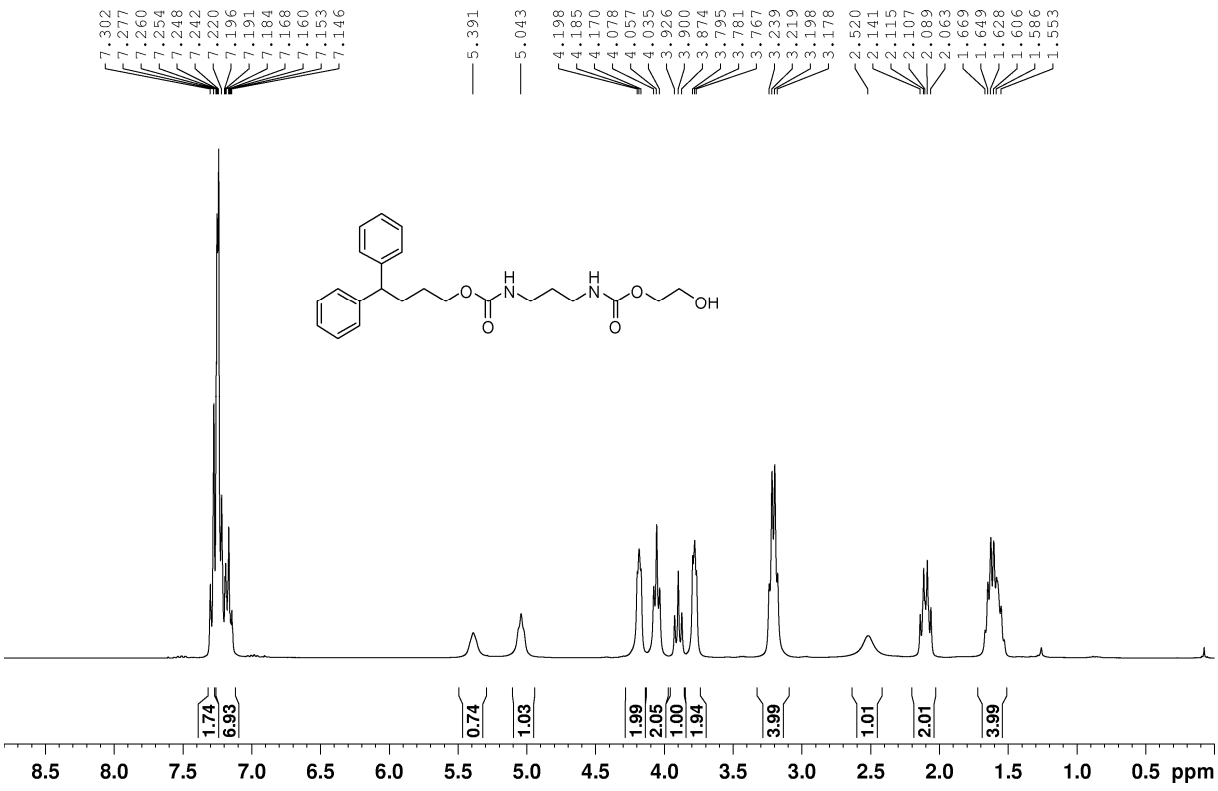
7.302
7.277
7.260
7.254
7.248
7.242
7.220
7.196
7.191
7.184
7.168
7.160
7.153
7.146
5.391
5.043
4.198
4.185
4.170
4.078
4.057
4.035
3.926
3.900
3.874
3.795
3.781
3.767
3.239
3.219
3.198
3.178
2.520
2.141
2.115
2.107
2.089
2.063
1.669
1.649
1.628
1.606
1.586
1.553
H
N
O
O
H
N
O
O
OH
1.74
6.93
0.74
1.03
1.99
2.05
1.00
1.94
3.99
1.01
2.01
3.99
8.5
8.0
7.5
7.0
6.5
6.0
5.5
5.0
4.5
4.0
3.5
3.0
2.5
2.0
1.5
1.0
0.5
ppm

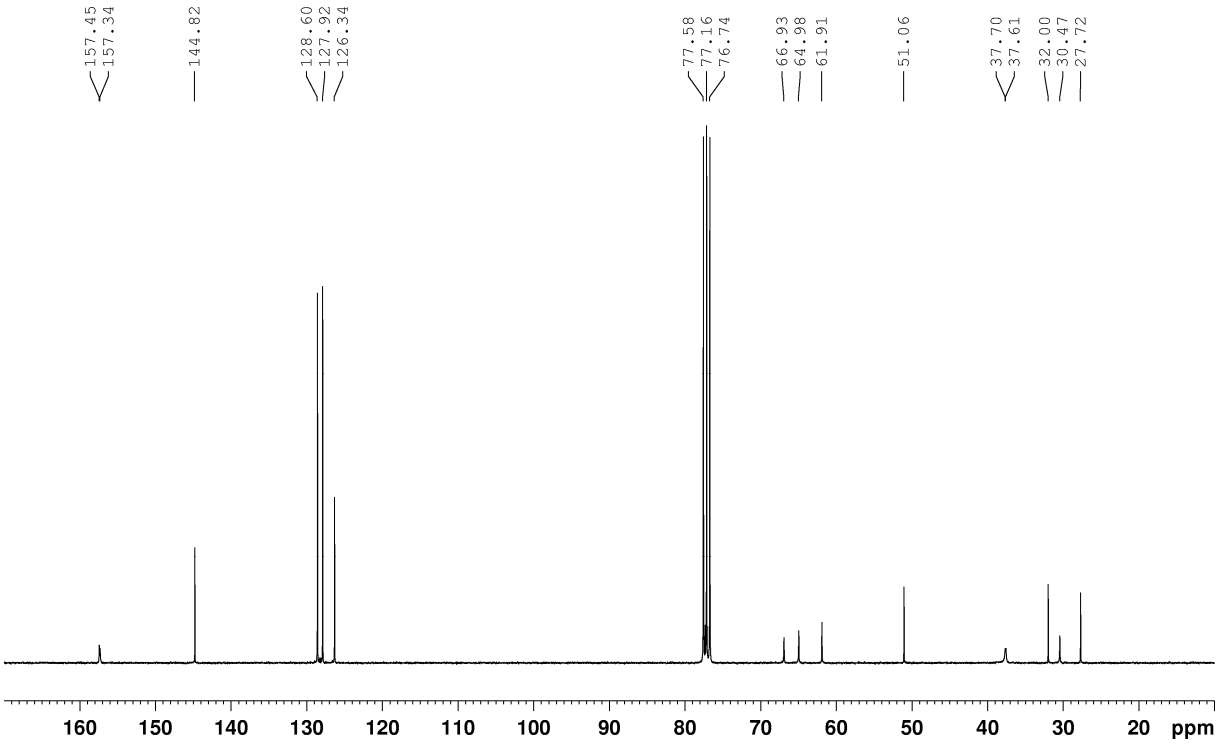
157.45
157.34
144.82
128.60
127.92
126.34
77.58
77.16
76.74
66.93
64.98
61.91
51.06
37.70
37.61
32.00
30.47
27.72
160
150
140
130
120
110
100
90
80
70
60
50
40
30
20
ppm

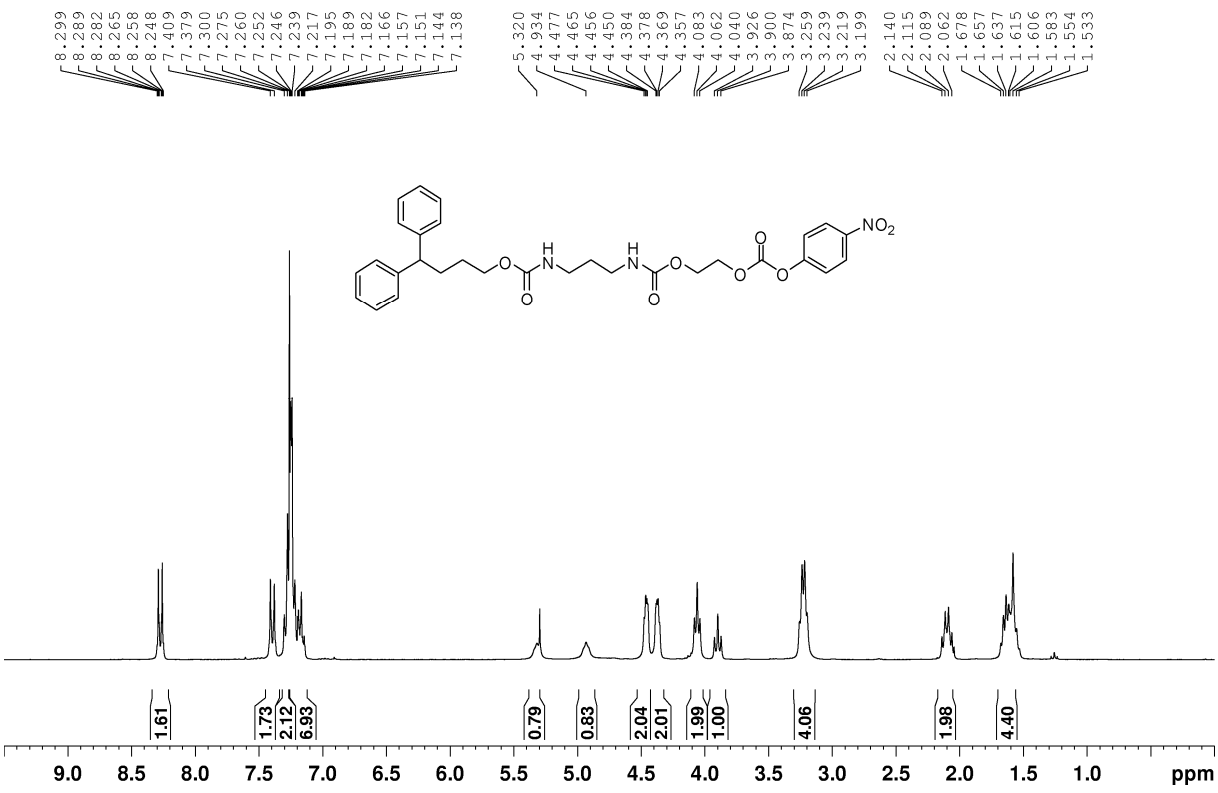
8.299
8.289
8.282
8.265
8.258
8.248
7.409
7.379
7.300
7.275
7.260
7.252
7.246
7.239
7.217
7.195
7.189
7.182
7.166
7.157
7.151
7.144
7.138
5.320
4.934
4.477
4.465
4.456
4.450
4.384
4.378
4.369
4.357
4.083
4.062
4.040
3.926
3.900
3.874
3.259
3.239
3.219
3.199
2.140
2.115
2.089
2.062
1.678
1.657
1.637
1.615
1.606
1.583
1.554
1.533
NO2
1.61
1.73
2.12
6.93
0.79
0.83
2.04
2.01
1.99
1.00
4.06
1.98
4.40
9.0
8.5
8.0
7.5
7.0
6.5
6.0
5.5
5.0
4.5
4.0
3.5
3.0
2.5
2.0
1.5
1.0
ppm

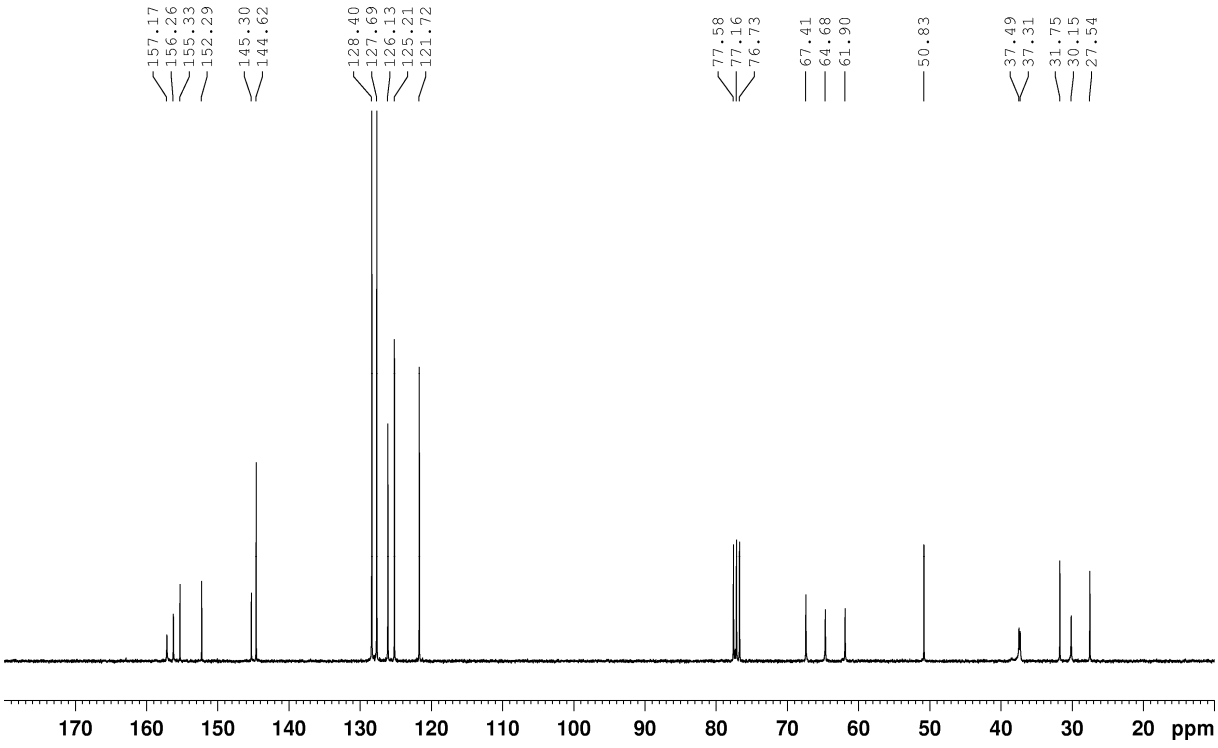
157.17
156.26
155.33
152.29
145.30
144.62
128.40
127.69
126.13
125.21
121.72
77.58
77.16
76.73
67.41
64.68
61.90
50.83
37.49
37.31
31.75
30.15
27.54
170
160
150
140
130
120
110
100
90
80
70
60
50
40
30
20
ppm

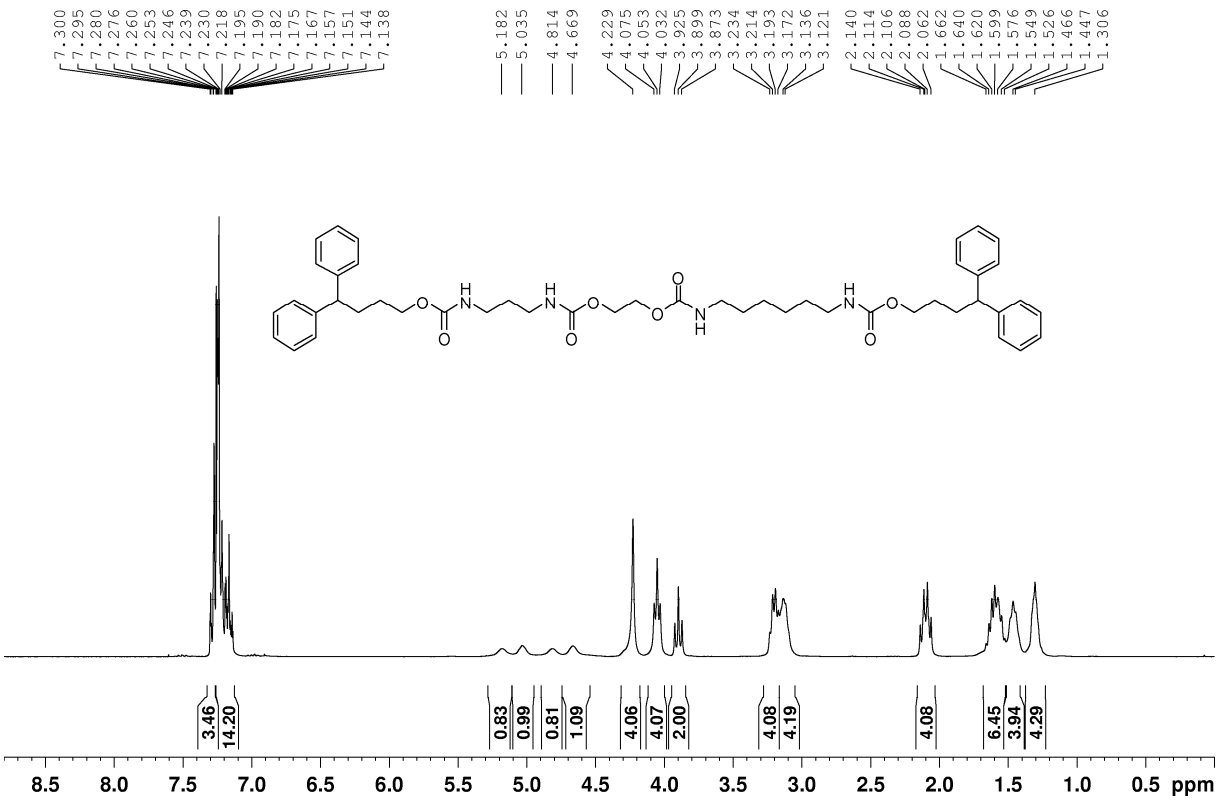
7.300
7.295
7.280
7.276
7.260
7.253
7.246
7.239
7.230
7.218
7.195
7.190
7.182
7.175
7.167
7.157
7.151
7.144
7.138
5.182
5.035
4.814
4.669
4.229
4.075
4.053
4.032
3.925
3.899
3.873
3.234
3.214
3.193
3.172
3.136
3.121
2.140
2.114
2.106
2.088
2.062
1.662
1.640
1.620
1.599
1.576
1.549
1.526
1.466
1.447
1.306
3.46
14.20
0.83
0.99
0.81
1.09
4.06
4.07
2.00
4.08
4.19
4.08
6.45
3.94
4.29
8.5
8.0
7.5
7.0
6.5
6.0
5.5
5.0
4.5
4.0
3.5
3.0
2.5
2.0
1.5
1.0
0.5
ppm

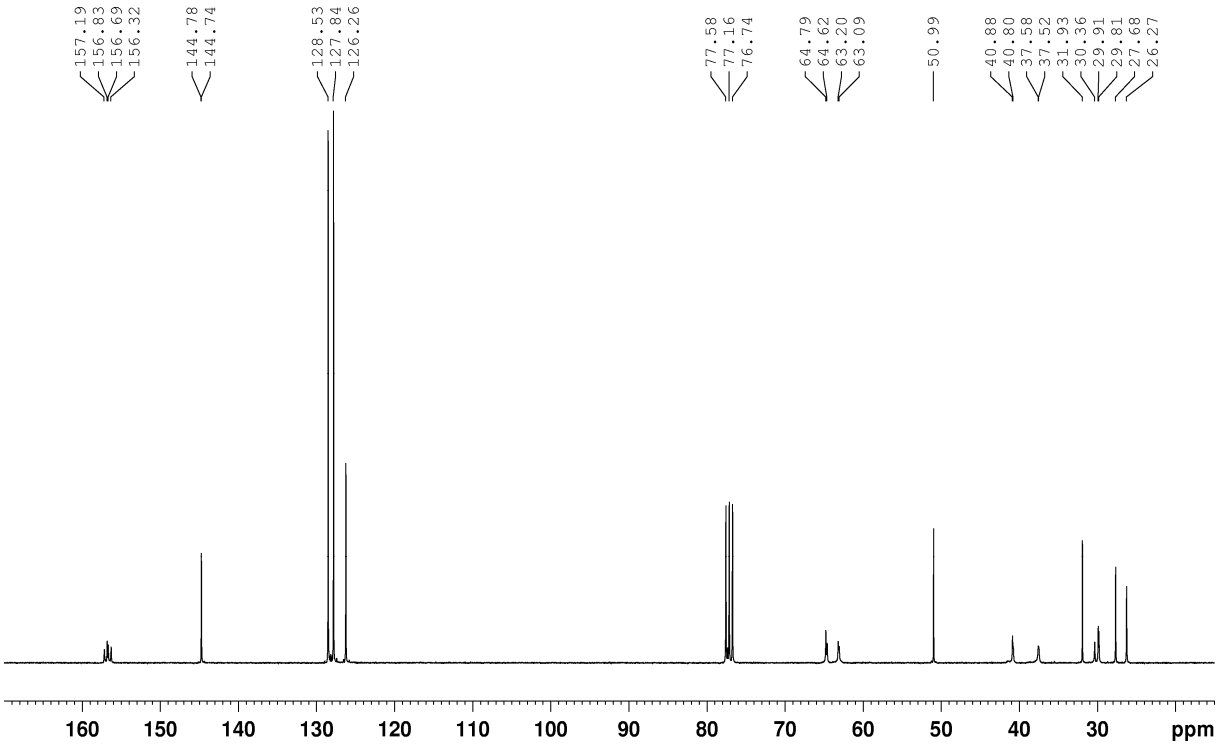
157.19
156.83
156.69
156.32
144.78
144.74
128.53
127.84
126.26
77.58
77.16
76.74
64.79
64.62
63.20
63.09
50.99
40.88
40.80
37.58
37.52
31.93
30.36
29.91
29.81
27.68
26.27
160
150
140
130
120
110
100
90
80
70
60
50
40
30
ppm